Jurnal Mekanikal
June 2013, No 36, 86-93

EVALUATING THE SURFACE PROPERTIES OF HYDROXYAPATITE COATING ON TITANIUM ALLOY SUBSTRATE

H. Hessam, S. Izman, S. Hamtaiepour

Faculty of Mechanical Engineering,
Universiti Teknologi Malaysia,
81310 Skudai, Malaysia

ABSTRACT

Surface morphology and surface roughness of substrate are important parameters that determine the quality of Sol-Gel coating. A variety of biomaterials such as metallic biomaterials are being used as implants in human body. In biomedical applications bioactive ceramic coatings such as hydroxyapatite (HA) are frequently used to modify the surface of the implant material. In the present work, HA coating on Ti-Zr-Nb alloy was done through sol-gel technique followed by sintering at temperatures of 500, 600, and 700˚C for 10 and 30 minutes. Analysis on the coating was done by surface roughness Ra *measurement, image analysis, and x-ray. It was found that optimum sintering was at temperature and time of 600^{o}C and 10 min.*

Keywords: *Heat treatment, Sol-Gel, Ti-Zr-Nb alloy, Surface roughness, Surface morphology*

1.0 INTRODUCTION

Bone injuries and failures often require the inception of the implants. A variety of bone implant materials, such as metals, polymeric materials, compositions and ceramics, are being explored for this purpose [1]. In particular, metallic implant materials, e.g. SUS316L stainless steel, Co-Cr-Mo-type alloys and titanium (Ti) and Ti alloys (e.g. Ti-Zr-Nb) are widely used as orthopedic and dental implant materials. Among these, Ti and some its alloy are preferred load-bearing implant materials due to their relatively low modulus, excellent strength-to-weight ratio, good fracture toughness and superior biocompatibility and corrosion resistance [2]. It has been demonstrated that Ti and some of its alloy are well accepted by human tissue compared to other metal materials [3]. Moreover, biological behavior research has demonstrated that Ti and zirconium (Zr) are favorable non-toxic metals with good biocompatibility. It has been reported that Zr is a metal with strong glass-forming ability and bulk amorphous Zi-based alloy exhibit high mechanical strength, high fracture toughness and good corrosion resistance [4].

Hydroxyapatite [$Ca_{10}(PO_4)_6(OH)_2$ or HA] is found to be the preferred coating due to its chemical, structural and biological similarity to human bones [5] and to its direct bonding capability to surrounding tissues [6]. HA coated titanium alloy implants integrate the bioactivity of HA and the mechanical properties of titanium alloy for a perfect combination. In addition, HA coating provides protection to the titanium alloy substrates against corrosion in the biological environment, and acts as a barrier against the release of toxic metal ions from the substrates into the living body [7]. Coating of HA and can be realized via thermal spraying [8], magnetron sputtering [9], pulsed laser deposition [10] and sol–gel dip coating [11]. In comparison, sol–gel method has the advantages of composition

Corresponding author : izman@fkm.utm.my

homogeneity, low cost, ease in operation and doping of ions thus is used widely, which is also the choice of method in this study.

Variable surface modification techniques can be used to produce desirable properties on surface of the material. Heat treatment is an important stage affecting the performance of Sol-gel coating. All activities are employed to reduce the cracks on the surface of coated layer. Temperature and time of heat treatment are mainly effect on coated surface layer. Smooth surface roughness of coating is important to reduce friction. Nevertheless, there are not many studies investigating the effect of these parameters especially on Ti-Zr-Nb alloy. In this present work effect of heat treatment parameters on Ti-Zr-Nb alloy using three different temperatures and two different times was investigated.

2.0 MATERIALS AND METHOD

2.1 Materials and Sample Preparation

Sample of a biomedical Ti-Zr-Nb alloy (ASTM F1713-96) in disc shape of 5 mm in diameter and 2 mm in thickness were cut from the as received bar. The main elemental composition is shown in Table 1. The sample was cut to form a disc and mounted by hardener/epoxy.

Table 1: Specification for Cobalt Chromium alloy (wt %)

Type [b]	Ti	Nb	Zr	Fe	C	N	H	O	other
Wrought alloy									
F1713-96	70-75	14	13.5	<1.0	<1.0	<0.03	<1.0	-	-

[a] Balance of composition is Titanium (Ti).
[b]ASTM specification F1713-96 standard specification for Wrought Titanium-73 Zirconium-14 Niobium-13.5 Alloy for surgical implants.

Aqueous solutions of $CaCl_2.2H_2O$ and $Na_3PO_4.12H_2O$ were prepared using double distilled H_2O. NaOH was added to the PO_4 precursor to control the PH at 10.5. These were mixed and adding the Ca precursor to the PO4 precursor ($10CaCl_2.2H_2O + 6Na_3PO_4.12H_2O + 2NaOH \rightarrow Ca_{10}(PO_4)_6(OH)_2 + 20NaCl + 92H_2O$. The precipitation reaction occurred immediately under stirring. The solution was then centrifuged for 5 mins at 4000 rpm for 4 times to remove the NaCl.

Ti-Zr-Nb substrates (diameter 5 mm and thickness 2 mm) were polished with SiC sandpapers grit 180, and then ultrasonically cleaned in acetone for 10 min, followed by rinsing with distilled water 2 times before dip-coating: the substrates were dipped into the sol with speed of 2cm/min; the coated substrates were dried at room temperature for one day and then sintered for 10 min and 30 min at 500, 600 and 700 °C. The coating process was repeated 2 times in order to obtain the required coatings thickness of 1.5 μm.

2.2 Field Emission Scanning Electron Microscopy (FESEM) Analysis

The FESEM instrument used was a SUPRA 35VP for analyzing the surface morphology of substrate after pretreatment. This machine is equipped with energy dispersive X-ray dispersion (EDAX) analysis.

2.3 Surface Roughness Analysis

The surface roughness substrates were measured using atomic force microscope (AFM). The arithmetic surface roughness *Ra* values were taken as the indicator of the surface roughness values.

3.0 RESULTS AND DISCUSSION

3.1 Surface Morphology Analysis

Surface morphologies of hydroxyapatite coating sintered at two different times and three different sintered temperatures are shown in Figure 1. Hydroxyapatite coating on Ti-Zr-Nb sintered at 500ºC showed a porous structure (Figures 1(e) and (f)). It is observed that by increasing of the sintering temperature from 500 to 600ºC the number of porosity decreased and denser structure was obtained (Figures 1(c) and 1(d)). But, by increasing of the sintering temperature from 600 to 700 ºC, some cracks were produced on the surface of hydroxyapatite. These cracks may lead to a decrease in mechanical properties of the coating layer.

Cracked surface of hydroxyapatite occurred for Ti-Zr-Nb sintered at 700ºC (Figures 1(a) and 1(b)). The difference in thermal expansion coefficients between Ti-Zr-Nb and the HA could be the reason for the crack occurrence. Due to higher thermal expansion coefficient of Ti-Zr-Nb compared to HA, the HA coating would be subjected to a tensile stress, causing the cracked surface.

High sintering temperature of 700ºC results in decomposition of HA structure. Also, it is shown that heat treatment at 600^{o}C for 10 min provides a crack free surface and dense structure.

3.2 Analysis of Surface Morphology

AFM results on surface roughness of hydroxyapatite coating on Ti-Zr-Nb are shown in Figure 2 and summarized in Table 2. It is found that by increasing the sintering temperature from 500 to 600^{o}C the number of porosity at the surface of the substrates decreased. This results in decrease in surface roughness of HA. This phenomenon can be observed from Figure 1(b). When the sintering was done at higher temperature (700ºC), higher Ra was resulted due to bigger HA grains. Higher surface roughness of HA coating on the Ti-Zr-Nb substrate is also due to the formation of thicker oxide layer during passivation in nitric acid. Further analysis on the microstructure revealed the presence of cracks in the HA sintered at higher temperature (Figure 3).

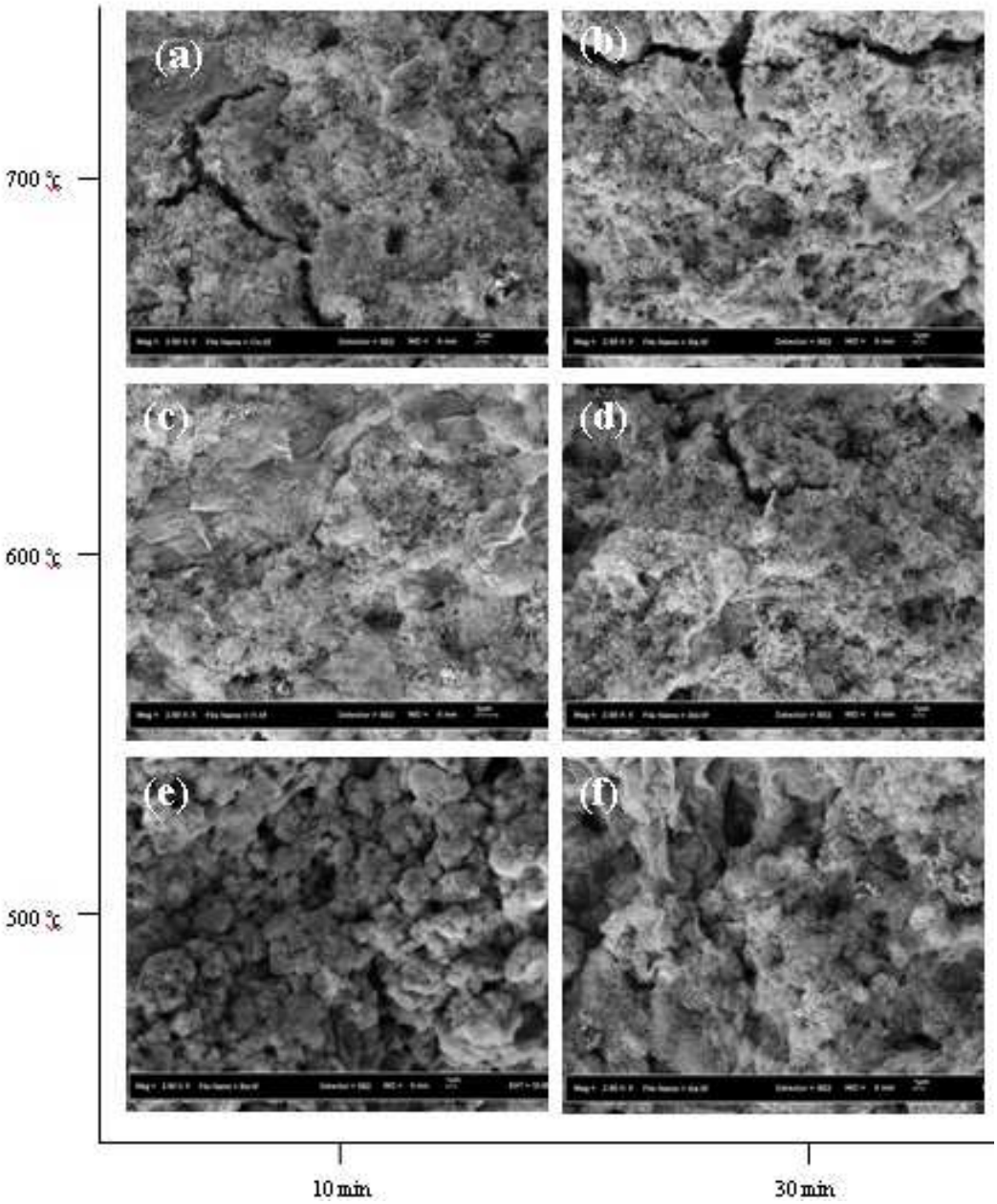

Figure 1: FESEM image of hydroxyapatite coating after sintering at, a) 500 ^{o}C and 10min, b) 500 ^{o}C and 30 min, c) 600 ^{o}C and 10 min, d) 600 ^{o}C and 30 min, e) 700 ^{o}C and 10 min, f) 700 ^{o}C and 30 min

Surface properties of implants such as surface roughness and its morphology strongly influence cell proliferation, cell attachment, and protein adsorption [12]. It means that smaller textures or three-dimensional topographic cause exposure of more surface area for interaction with biomaterials. In this regard, it can be said that HA coating sintered at 600°C and 10 min for Ti alloys shows optimum results in terms of surface roughness.

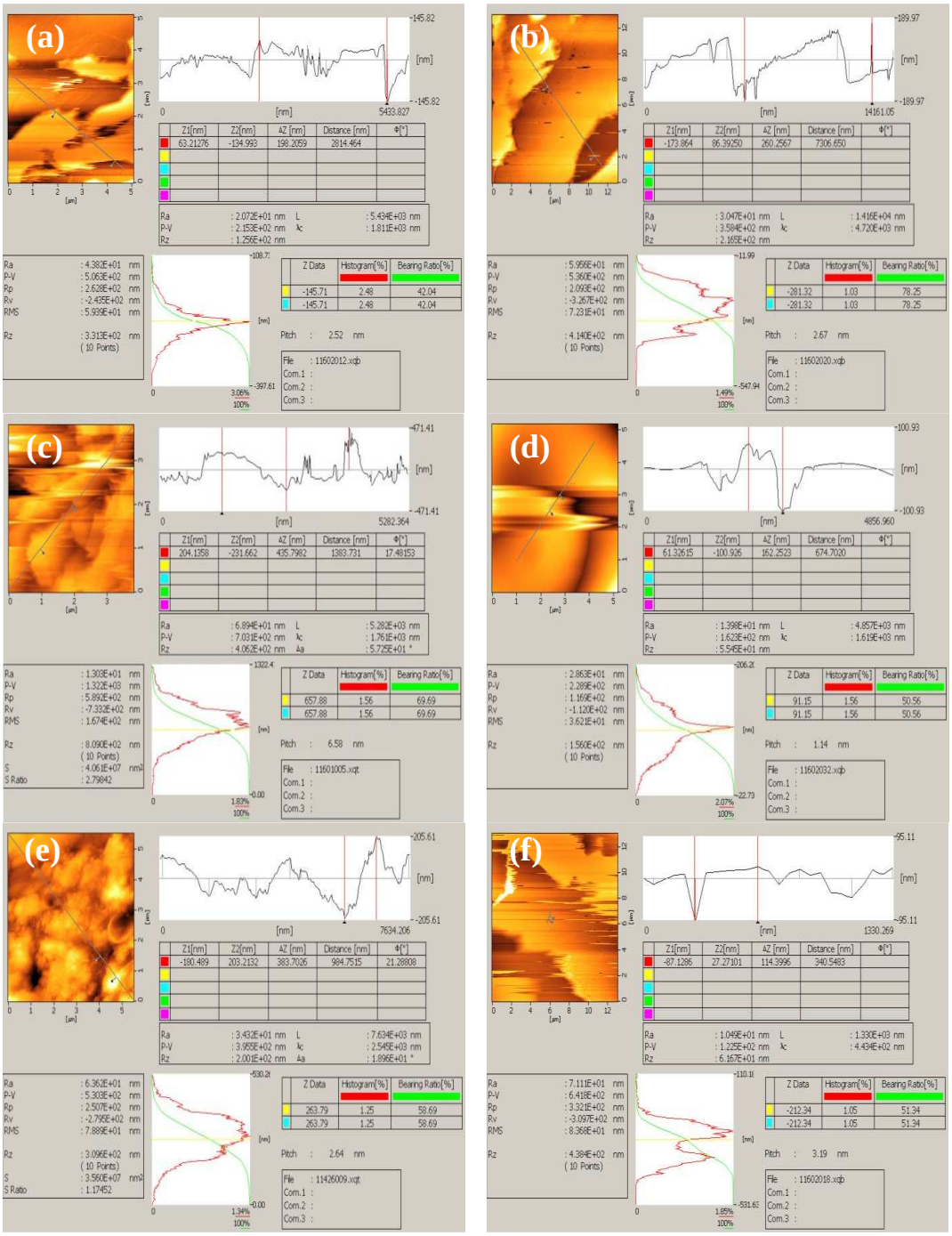

Figure 2: AFM results of hydroxyapatite coating on Ti-6Al-4V sintered at, a) 500ºC and 10 min, b) 500ºC and 30 min, c) 600ºC and 10 min, d) 600ºC and 30 min, e) 700ºC and 10 min, f) 700ºC and 30 min

Table 2: Surface roughness Ra measured by AFM (nm)

Time	Heat treatment temperature		
	500 °C	**600 °C**	**700 °C**
10 min	43.8	13.09	63.6
30 min	59.5	28.6	71.1

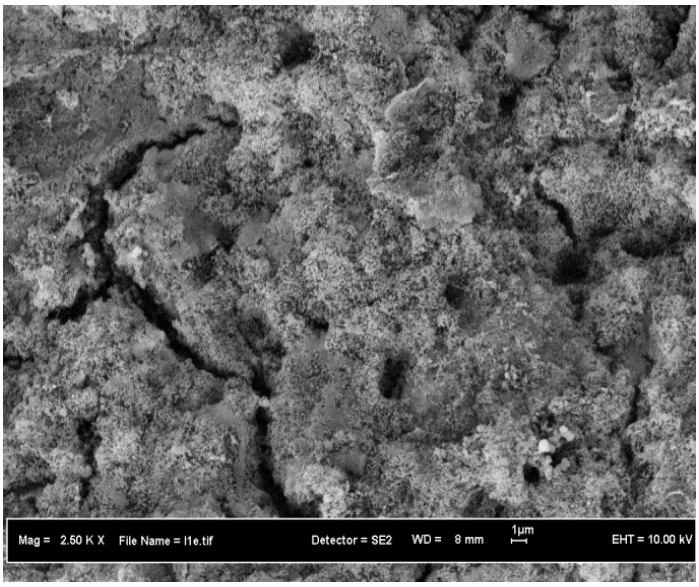

Figure 3: Cracked surface of hydroxyapatite coating on Ti-Zr-Nb sintered at 700ºC.

The EDAX analysis of hydroxyapatite coating on Ti-Zr-Nb sintered at 600ºC and 10 min evidenced carbon contamination on the surface. It remained on the coating surface from precursors or solvents (Figure 4).

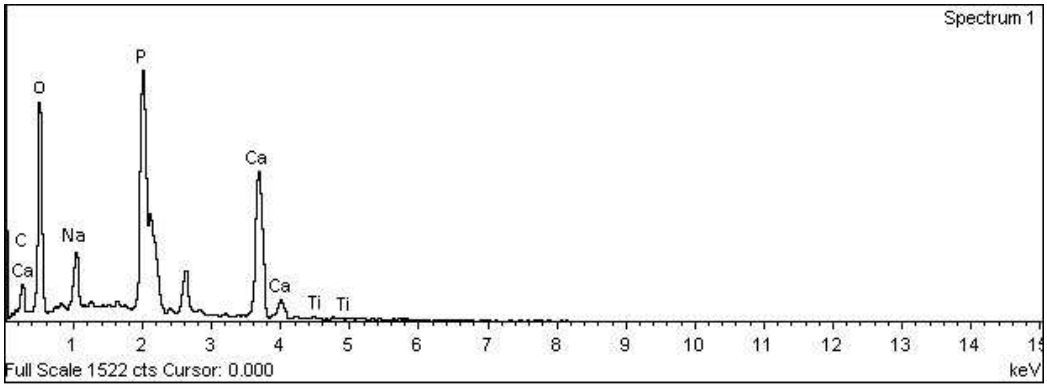

Figure 4: EDAX analysis of hydroxyapatite coating over Ti-Zr-Nb sintered at 600ºC and 10 min

Figure 5 illustrates XRD patterns of hydroxyapatite coating on Ti-Zr-Nb. XRD patterns show the presence of TCP (which is biodegradable *in vivo*) and CaO due to ion migration from the metallic substrates into the coating layer. Some characteristic peaks of HA and TCP phase are observed to be between 20 to 50° of 2θ. The peaks related to the CaO phase are also appeared to be at 30º, between 40-45º and 55-60º of 2θ. The strongest peaks of HA are shown to be at 29º and 31º of 2θ.

The reaction and presence of *β*-TCP and CaO may explain by the following equation:

$$Ca_{10}(PO_4)_6(OH)_2 \rightarrow 2\beta\text{-}Ca_3(PO_4)_2 + Ca_3(PO_4)_2 \cdot CaO + 2H_2O$$

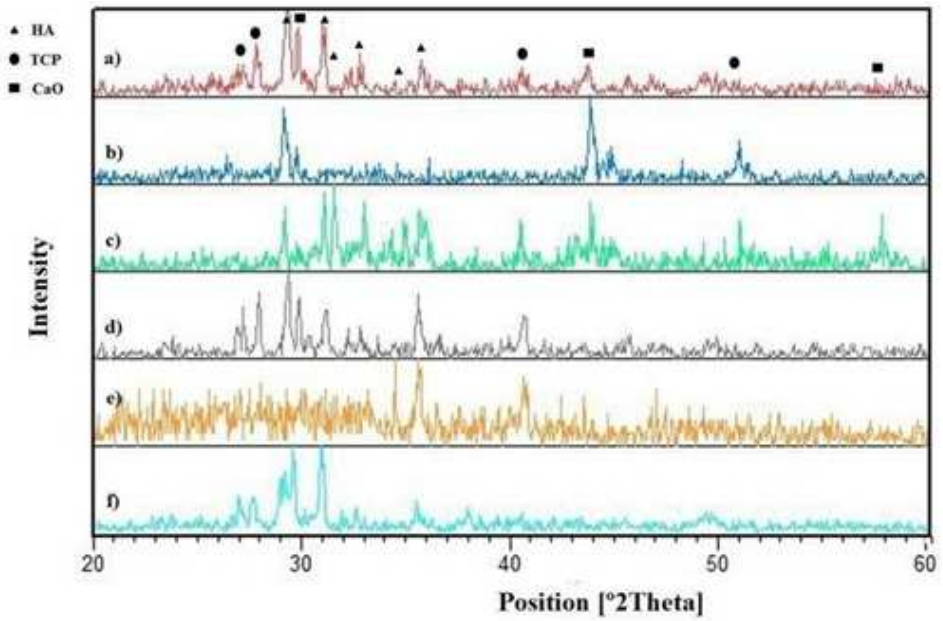

Figure 5: XRD graphs of hydroxyapatite coating on Ti-Zr-Nb at different sintered temperature and time: a) 500 ^{o}C 10min, b) 500 ^{o}C 30min, c) 600 ^{o}C 10min, d) 600 ^{o}C 30min e) 700 ^{o}C 10min and f) 700 ^{o}C 30min

4.0 CONCLUSIONS

The following conclusions can be drawn from this preliminary study on the effect of heat treatment parameters on HA coating on Ti alloy substrate:

a) FESEM observation showed that by increasing of the sintering temperature from 500ºC to 600ºC the number of porosity decreases and denser structure obtained for Ti-Zr-Nb substrates. Sintered hydroxyapatite coating at 700ºC for 10 and 30 min showed higher surface roughness and occurrence of cracks.

b) AFM analysis showed that by increasing sintering temperature up to 600^{o}C surface roughness of hydroxyapatite coating is decreased and smoother surface is obtained. It is believed that the porosity decreases when temperature increased from 500 to 600^{o}C.

c) The optimum sintering was obtained at temperature and time of 600^{o}C and 10 min. This condition provides a crack free surface on the sol-gel coated substrates.

ACKNOWLEDGEMENTS

Authors would like to express highest gratitude to Ministry of Higher Education, Malaysia and Universiti Teknologi Malaysia for funding via project vote nos. 78611 and Q.J130000.7124.02H60.

REFERENCES

1. Niinomi M. Fatigue performance and cyto-toxicity of low rigidity titanium alloy, Ti–29Nb–13Ta–4.6Zr. Biomaterials 24 (2003) 2673
2. Wen CE, Yamada Y, Hodgson PD. Fabrication of novel alloy foams for biomedical applications. Mater Forum 29 (2005) 274
3. Niinomi M, Akahori T, Takeuchi T, Katsura S. Dental precision casting of Ti-29Nb–13Ta–4.6Zr using calcia mold. Mater Sci Forum 475-479 (2005) 2303
4. Y. Wang, S. Zhang, X. Zeng, K. Cheng, M. Qian, W. Weng, Mater. Sci. Eng. 27 (2007) 244
5. M. Sivakumar, I. Manjubala, Mater. Lett. 50 (2010) 199
6. R.R. Kumar, M. Wang, Mater. Lett. 55 (2002) 133
7. M. Cavalli, G. Gnappi, A. Montenero, D. Bersani, P.P. Lottici, S. Kaciulis, G. Mattogno, M. Fini, J. Mater. Sci. 36 (2008) 3253
8. K.A. Khor, P. Cheang, J. Mater. Process. Technol. 63 (1997) 271
9. T.G. Nieh, A.F. Jankowski, J. Koike, J. Mater. Res. 16 (2001) 3238
10. Q.H. Bao, C.Z. Chen, D.G. Wang, Q.M. Ji, T.Q. Lei, Appl. Surf. Sci. 252 (2005) 1538.
11. K. Cheng, G.R. Han, W.J. Weng, H.B. Qu, P.Y. Du, G. Shen, J. Yang, J.M.F. Feireira, Mater. Res. Bull. 38 (2003) 89.
12. A.V. Singh, V. Vyas, R. Patil, V. Sharma, P.E. Scopelliti, G. Bongiorno, A. Podestà, C. Lenardi, W.N. Gade, P. Milani, PLoS ONE 6 (2011) e25029